

PAPER • OPEN ACCESS

Preparation and Characterization of Biochars from Plant and Animal Waste Under Different Pyrolysis Temperature

To cite this article: Mustafa Hussein Ali and Alaa Hasan Fahmi 2024 *IOP Conf. Ser.: Earth Environ. Sci.* **1371** 082029

View the [article online](#) for updates and enhancements.

You may also like

- [Where should we apply biochar?](#)
Hamze Dokoohaki, Fernando E Miguez, David Laird et al.
- [Preparation and characterisation of graphitic biochar materials derived from rose oil industry waste via different pyrolysis durations and ball milling for advanced composites](#)
Saleh M Alluqmani, Hissah Saedoon Albaqawi, Musaed A Hakami et al.
- [The effect of dispensing biochar of palm oil empty bunches and palm oil fronds on the population of soil organisms](#)
N A Lubis, B Hidayat, T Sabrina et al.

PRIMETM
PACIFIC RIM MEETING
ON ELECTROCHEMICAL
AND SOLID STATE SCIENCE

HONOLULU, HI
October 6-11, 2024

Joint International Meeting of
The Electrochemical Society of Japan (ECSJ)
The Korean Electrochemical Society (KECS)
The Electrochemical Society (ECS)

Early Registration Deadline:
September 3, 2024

**MAKE YOUR PLANS
NOW!**

Preparation and Characterization of Biochars from Plant and Animal Waste Under Different Pyrolysis Temperature

Mustafa Hussein Ali¹ and Alaa Hasan Fahmi²

^{1,2}Department of Soil Science and Water Recourses, College of Agriculture, University of Diyala, Diyala, Iraq.

¹E-mail: mustafahussein989898@gmail.com

Abstract. Biochar is widely used for environmental and agricultural purposes due to its positive effect on soil fertility, immobilization of pollutants and sequestration of carbon. This research produced biochar from plant waste (palm fronds PFB) and animal waste (sheep manure SMB) at different pyrolysis temperatures (300 and 700 °C) and compared their physicochemical properties. The results showed the biochars produced at a low temperature (300 °C) had higher yield. However, the increasing pyrolysis temperature led to increased surface area, pore volume, EC, pH, ash content, carbon content, and negative zeta potential. Sheep manure biochar (SMB) was higher elements (phosphorus, potassium, calcium). Therefore, it can be suggested to use sheep manure biochar as organic fertilizer for soil treatment rather than used for the removal of contaminants as preferred for palm fronds biochar produced at higher pyrolysis temperatures depending on their properties.

Keywords. Biochar, Pyrolysis, Physicochemical properties, Sheep Manure, Fronds feed stocks.

1. Introduction

Biochar is the byproduct of low-oxygen pyrolysis of biomass such as food scraps, animal manure, and tree leaves. Biochar is mainly composed of carbon, but it also has smaller amounts of other elements, such as oxygen, hydrogen, sulfur, and nitrogen [1,2]. Biochar has many applications, including as a soil fertilizer, maintaining soil carbon content, and reducing greenhouse gas emissions. In addition, it can be used as a low-cost adsorbent to remove organic and inorganic pollutants from contaminated water and soil [3,4]. Previous studies reported that it can be applied to improve soil structure, and soil acidity, and increase the soil's ability to retain water. In addition to stimulating soil microscopic renaissance [5,6].

The physical and chemical properties of biochar, such as high surface area, number of pores, abundance of functional aggregates, mineral content, etc., increase the effectiveness of biochar as an adsorbent for wastewater purification [7]. Biochar's properties determine its uses. The properties of biochar directly depend on the raw materials and conditions of its preparation. Depending on these factors, different types of biochar are available in their chemical and physical properties, allowing for the diversity of their applications, such as safe fertilizers or adsorbents for pollutant removal and other applications [8,9].

Ippolito et al [10] to utilizing approximately 5,400 peer-reviewed journal articles and over 50,800 individual data points, feedstock selection has the largest influence on biochar properties. Specific



surface area is greatest in wood-based biochars, which, in combination with pyrolysis temperature, could likely promote greater changes in soil physical characteristics over other feedstock-based biochars. This could potentially lead to longer-term changes in soil nutrient retention. One can reasonably predict the availability of various biochar nutrients (e.g., N, P, K, Ca, Mg, Fe, and Cu) based on feedstock choice and total nutrient content. Results can be used to create designer biochars to help solve environmental issues and supply a variety of plant-available nutrients for crop growth.

Of the waste available locally in Iraq (sheep manure and palm fronds), the number of palm trees in Iraq reached 22 million palm trees in the year 2022, providing 3 million tons annually of waste, and the number of sheep reached 6,604,185, providing 450 thousand tons annually of manure [11]. Therefore, this study aimed to sustainably manage local waste, whether from animals or plants, to produce biochar under different pyrolysis temperatures (300 and 700 °C) and their physiochemical properties were analyzed. It provides a comprehensive description of the characteristics of each type of biochar, and provides an insight into its suitability for various applications, such as enhancing soil fertility or reducing pollution by treating contaminated water and soil.

2. Materials and Methods

2.1. Feedstock's and Pyrolysis

Samples of palm fronds (PF) and sheep manure (SM) were collected from the farm at Diyala state, Iraq. The two samples were air-dried, then impurities were removed from them and cut into small parts (2 cm³). The prepared samples were placed in ceramic crucibles with a suitable lid and subjected to the furnace (Nabentherm type Furnace 1300°C. °C, 400 V, 50/60 Hz Germany) for pyrolysis at temperatures (300°C and 700°C) for two hours Fig.1,. After pyrolysis, all biochar samples were ground, passed through a 50-µm sieve as suggested by Fahmi et al. [12], and stored in glass beakers at room temperature before analysis.

Biochar derived from palm fronds was then classified as PFB-300 and PFB-700 produced at 300°C and 700°C, respectively. While biochar produced from sheep manure was classified as SMB-300 and SMB-700, produced at 300°C and 700°C, respectively. Biochar productivity was calculated as in equation [12],

$$\text{Biochar yield (\%)} = (\text{Mass of biochar g}) / (\text{Oven dry mass of feedstocks g}) \times 100 (\%) \quad (1)$$

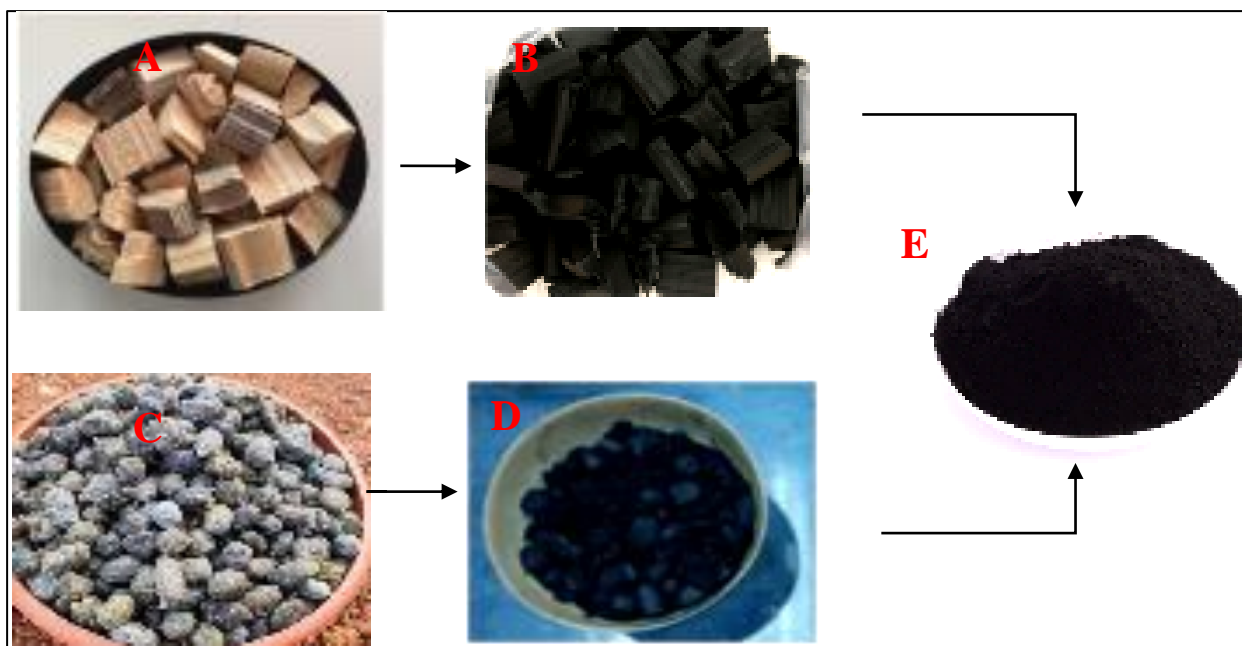


Figure1. A. frond feedstock, B. frond biochar, C. sheep feedstock, D. sheep biochar, E. biochar powder.

2.2. Characterization of Biochars

2.2.1. (PH) and Electrical Conductivities (EC)

The pH of the biochar was analyzed following the method presented by [13]. About 4.0 g of biochar was placed with 100 mL of distilled water in a conical flask, covered with glass, and boiled for 5 minutes. After letting it cool, the pH was measured using a pH meter (Bp3001, Germany).

To measure electrical conductivity (EC), the biochar was placed in distilled water with a solid-to-liquid ratio of 1,5, shaken for 24 hours, and then the electrical conductivity was measured using an EC meter (HANNA instrument).

2.2.2. Element Analysis (CHNS)

The content of carbon (C), hydrogen (H), nitrogen (N), and sulfur (S) in the biochar were analyzed using atruspec CHN analyses. The oxygen content (O) was determined using equation (2). These results were used to calculate the atomic ratios of H/C and O/C, facilitating the evaluation of the relationship between the pyrolysis temperature and the relative degree of aromaticity (H/C ratio) and polarity (O/C) of each biochar, as demonstrated in the equation below [14]:

$$O(\%)=100\% - (\%C + \%H + \%N+\%S) \quad (2)$$

2.2.3. Fourier-transform Infrared Spectroscopy (FTIR)

Biochars were analyzed using Fourier transform infrared spectroscopy to identify functional groups. We used a Shimadzu 1800, a Japanese instrument, to analyze spectra in the 400–4000 cm^{-1} region after pressing samples combined with KBr into translucent sheets.

2.2.4. Ash Content

By employing the dry combustion method, we were able to ascertain the biochar's ash composition. For this procedure, you'll need to bake 5 grams of biochar at 500 degrees Celsius for 8 hours, let the crucible cool, and then weigh it. To get the ash percentage, which allows for a precise evaluation of the ash content, we subtracted the sample's beginning weight from its end weight in Equation (3) [15].

$$\text{Ash content}(\%) = (\text{Weight of ash (g)}) / (\text{Dry mass of biochar (g)}) \times 100\% \quad (3)$$

2.2.5. Zeta Potential

To create a suspension with a concentration of 0.5 g L⁻¹, 200 mL of distilled water was added to 0.1 g of finely processed biochar powder in a conical flask. For 12 hours, the flask was mixed by spinning it at 150 revolutions per minute. Next, we used the Malvern Panalytica zeta potential scale to determine the biochar suspension's zeta potential [16].

2.2.6. Physical Analysis of Biochars

2.2.6.1. Field Emission Scanning Electron Microscopy (FESEM) and Energy-Dispersive X-Ray (EDX) Analysis

(FESEM) is a high-resolution method that analyzes biochar surfaces at the nanoscale scale by performing morphological analysis using a field emission electron beam. Delivers comprehensive three-dimensional pictures of biochar samples. When used in tandem with field emission scanning electron microscopy (FESEM), energy dispersive X-ray spectroscopy (EDX) measures the X-ray energy produced by the sample beam's interaction with the electron to determine the chemical composition. This allows the identification and measurement of the chemical elements present in the samples. Using MIRA III FESEM (scanning electron microscope, Czech), ensuring comprehensive characterization of all samples.

2.2.6.2. The Surface Area

The surface area of the samples was evaluated by the Brunauer-Emmett-Teller (BET) technique, which uses N₂ adsorption at 77K and using BELSORP MINI II (Japan). Total surface area was

determined using the multipoint BET method, while microspore surface area was calculated using the t-plot method. Pore sizes were evaluated using the Barrett-Joyner-Halenda (BJH) method based on adsorption isotherms, with the total pore volume derived from a single N₂ adsorption point at a relative pressure (P/P₀) of 0.99.

3. Results and Discussion

3.1. Biochar Yield

Table 1 presents the biochar yield at different pyrolysis temperatures. An increase from 300 °C to 700 °C resulted in a decrease in biochar yield. The PFB biochar peaked at 44.85% at 300 °C, and decreased to 26.27% at 700 °C, while SMB biochar reached its highest yield of 61.57% at 300 °C, and decreased to 38.42% at 700 °C.

Animal manure biochar yields are typically higher compared to plant biomass due to the higher non-volatile ash content, with yields ranging between 40% and 60%, depending on conditions and type of compost, while wood yields are generally lower (20%-30%). These results are consistent with previous study [17].

Biochar formation requires stages such as partial and complete hemicellulose hydrolysis, partial and complete cellulose hydrolysis, and high carbonization process. The decrease in biochar yield at high temperatures for both PFB and SMB samples is attributed to gas volatilization, including CO₂, NH₃, CO, H₂O, and HCN, which leads to lower biochar yield [18].

3.2. Ash Content

Table 1 displays the ash contents of biochar produced at various pyrolysis temperatures. The findings indicate a rise in biochar ash content with increasing pyrolysis temperature, as expected due to enhanced volatilization during pyrolysis, leading to char with higher carbon content. Specifically, the ash content percentages were 55.14% and 73.7% for PFB-300 and PFB-700, respectively. For SMB, they were 38.42% and 62.28% for SMB-300 and SMB-700, respectively.

Generally, the augmented ash content results from decreased levels of other elements during pyrolysis. Elements such as C, H, N, O, and S are volatilized during heating, while inorganic salts like quartz and calcite remain unvolatilized. According to [19,12]. the escalating ash content in biochar with increasing pyrolysis temperature is attributed to the progressive mineral concentration and the destructive volatilization of lignocellulosic materials.

3.3. BET Surface Area

With increasing pyrolysis temperature, the surface area and number of pore volume increased significantly. The highest surface area was for PFB-700 (247.77) m² g⁻¹, followed by SMB-700 (89.885) m² g⁻¹ and for PFB-300, and SMB-300 were 20.608, and 17.072 m² g⁻¹, respectively. This was due to the permeation of hemicellulose and the rupture of many organic materials, and thus many pores were produced inside the biochar. Thus, there was a direct relationship between the increase in pyrolysis temperature and the surface area, and this was consistent with result of study by Zhang et al. [20].

The total pore volume (p/p₀) showed an increase with increased temperature. The total pore volume (p/p₀) for PFB-300 and PFB-700 were 0.028573 cm³ g⁻¹, and 0.1766 cm³ g⁻¹, respectively. For SMB-300 and SMB-700 were recorded as 0.056674 cm³ g⁻¹, and 0.1359 cm³ g⁻¹, respectively, as show in Table (1).

These observations are consistent with the findings of [21], which indicates that raised the pyrolysis temperature develops pore properties, by discharging volatile organic materials, which leads to the destruction of the pore wall and raises the total pore volume within the biochar, which was consistent with their found [22]. Both SMB-700 and PFB-700 exhibit large surface area and total pore volume as well as numerous cavities on the surface making it a prime candidate for water and soil purification endeavors by adsorption of cationic chemicals and organic contaminants[23].

Table 1. Physical properties of Biochar produced from Palm Fronds (PFB) and Sheep Manure (SMB) at different pyrolysis temperatures.

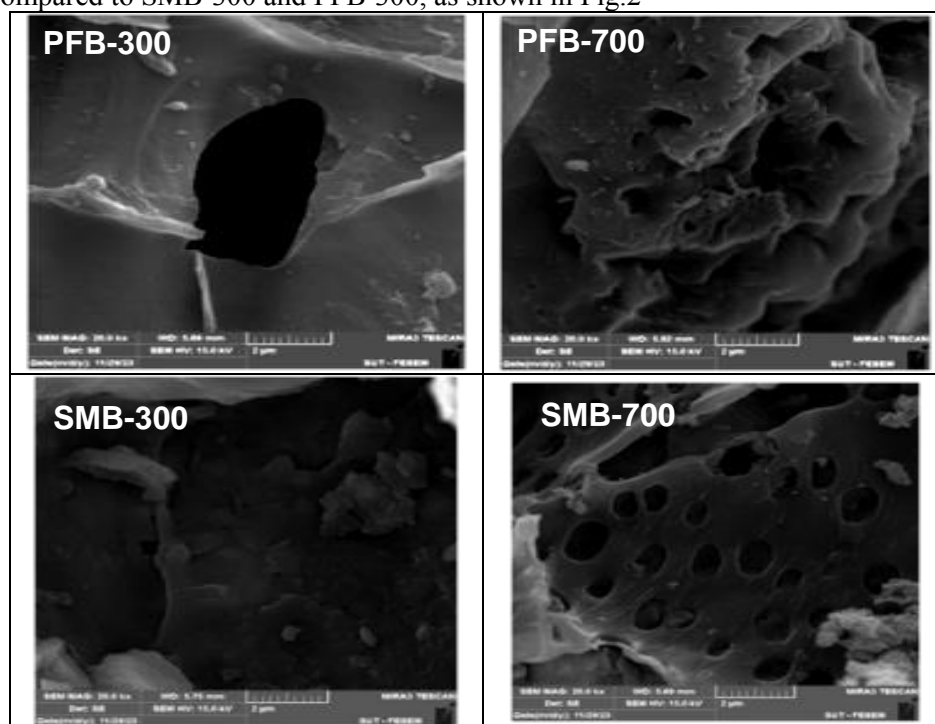
Physical Properties	PFB		SMB	
	300 °C	700 °C	300 °C	700 °C
Yield (%)	44.85	26.27	61.57	37.71
Ash content (%)	55.14	73.7	38.42	62.28
BET surface area (m ² g ⁻¹)	20.608	247.77	17.072	89.885
Total pore volume (p/p0=0.990) (cm ³ g ⁻¹)	0.028573	0.1766	0.056674	0.1359

3.4. Field Emission Scanning Electron Microscopy (FESEM)

Examining the morphological characteristics of solid surfaces plays an important role in diagnosing structural design and distinguishing deformations. Microscopy at $\times 20,000$ magnification revealed the pore structure of four samples. The internal pores represented in Fig. 2 (PFB-300) indicate the presence of cellulose, hemicellulose and lignin, which were converted into porous and amorphous after heat treatment. This led to channel formation and surface development at 300°C pyrolysis temperature. To a certain extent,

when the pyrolysis temperature was raised to 700°C, the amount and size of pores and surface area increased, and cavities, cracks and small pits also appeared, as can be seen from Fig.2 (PFB-700). From a chemical standpoint, it must be noted that the presence of many small and medium-sized pores on these surfaces is one of the factors responsible for their effectiveness in removing heavy metals [23]. These results are consistent with a study that showed the volume of small pores, the total pore volume, and the surface area increased, and the surface effectiveness of biochar increased with increasing temperature[24,25].

As for the sheep manure samples, they also showed a significant response to high degrees of pyrolysis, as Fig.2 (SMB-700) showed a well-developed, heterogeneous structure with very high porosity. This development could be due to the escape of volatiles during high-temperature decomposition [26]. These results were consistent with a study that used the same raw material [27]. These results are consistent with BET analysis confirming the increased surface area and pore density of SMB-700 and PFB-700 compared to SMB-300 and PFB-300, as shown in Fig.2

**Figure 2.** FESEM images of biochar PFB and SMB at 300°C and 700 °C.

3.5. Fourier-Transform Infrared Spectroscopy (FTIR)

It is an analytical technique used to identify the content of materials the chemical group functions by using an infrared spectrum. From the Fig.3 of biochar FTIR data shows the different peaks of SMB-700 and SMB-300 corresponding to stretching the O-H broad band at 3444 cm^{-1} in SMB-300, throughout the increasing of temperature to 700°C the stretching O-H band start to slowly diminish. This was expected due to the mass loss during thermal decomposition and gas product evolution [27].

The peak 2939 cm^{-1} in SMB-300 biochar shows sharper peak 2879 cm^{-1} as the temperature increased in SMB-700 biochar which belong to the stretching vibration of C-H, the absorption peaks at 1616 cm^{-1} and 1423 cm^{-1} in SMB700 and SMB-300 biochars is attributed to the stretching vibration of C=C and C=O [28]. The peak 1089 cm^{-1} of SMB-300 biochar associated with C-O vibrations in esters and ethers and the same for SMB-700 biochar peak 1035 cm^{-1} [29]. The absorption peak of 873 cm^{-1} in both SHB-300 and SHB-700 biochars is attributed to the bending vibration of C-H on the aromatic ring [27, 28].

FTIR spectrum of PFB-300 biochar shows peaks at 3441 cm^{-1} which obtained to be sharper peak at 3410 cm^{-1} as the temperature increased in PFB-700 attributable to the stretching O-H possibly from carboxyl, phenol, and alcohol functional groups [30]. We also notice the distinctive C-H stretching vibration of the alkyl structure of aliphatic groups at 2877 cm^{-1} for PFB-700 but not for the PFB-300 [24,31,32]. The band at $1697\text{--}1512\text{ cm}^{-1}$ in both PFB-300 and PFB-700 biochar sample due to the presence of aromatic C=C and C=O stretching vibration represented possible conjugated ketones 1600 cm^{-1} [33,34]. A peak of C-O stretching is also presented in the sample at 1149 cm^{-1} and 1168 cm^{-1} for PFB-300 and PFB-700, respectively [35].

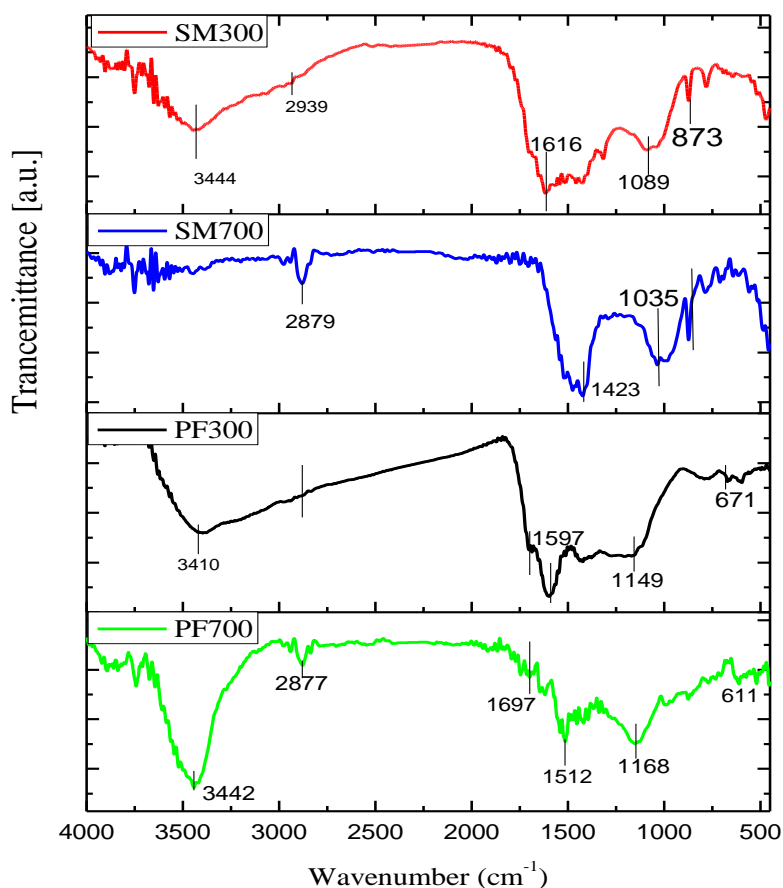


Figure 3. FTIR spectra peak of PFB and SMB at 300°C and 700°C .

3.6. PH

By observing Table 2, we note that the heat of pyrolysis of biomass controls the development of alkaline pH due to the formation of insoluble salts that are mostly more abundant in hardwood [36]. Moreover, the decomposition of organic acids present in biochar with increasing pyrolysis temperature to less acidic acids. It increased the alkaline pH of both PFB and SMB. At temperatures of 700 °C, consistent with the increase in ash content, as shown in Table 1. These results are consistent with previous studies [37,38,39], with this variation in pH depending on the type of feedstocks and the intensity of pyrolysis.

It should be noted that the pH of PFB-300 and PFB-700 are 1 and 1.4 pH units lower, respectively, than SMB-300 and SMB-700, despite being subjected to the same pyrolysis conditions, which is due to wood-derived biochar being less acidic than other materials. This supports findings [40,41], that non-wood biochar typically exhibits higher pH levels compared to wood-derived biochar. It should be noted that biochar produced at 300 °C, especially PFB, exhibits a low pH (6.4), which makes it suitable for fertilizing alkaline soils without causing the soil pH to rise.

3.7. Electrical Conductivity (EC)

The electrical conductivity ranges from 6.41 to 7.6 dS m⁻¹ for PFB-300, and SMB-300, and from 8.2-16.3 dS m⁻¹ for SMB-700 and PFB-700, respectively (Table 2). The increase of electrical conductivity with increasing temperature with corresponding increases in ash content and pH. Both the feedstock type and pyrolysis temperature significantly affect the chemical and physical attributes of biochar [42,10]. In addition, the electrical conductivity of biochar tends to increase with higher pyrolysis temperatures within each feedstock, consistent with previous research results [17,43,44].

We note that biochar derived from palm fronds at a temperature of 700 °C has the highest electrical conductivity. This indicates its high content of water-soluble ions [45] and confirmed with results in Table 2. So both biochar SMB-300 and PFB-300 have low electrical conductivity, they are often used in soil improvement and agricultural fertilizer applications. They can also be used to purify water and air from pollutants. As for both SMB-700 and PFB-700, they have high electrical conductivity, which makes them an effective choice for generating clean energy [46].

3.8. Zeta Potential

Variations in zeta potentials (PZC values) were observed across different pyrolysis temperatures, as shown in Table 3 (-2.96 mV for PFB-300, -6.12 mV for PFB-700, -8.01 mV for SMB--300, and -8.39 mV for SM--700) respectively. All biochars showed negative zeta potentials, indicating the presence of negative surface charges (as shown in Table 2).

This increase in passivity at higher pyrolysis temperatures is attributed to the increase in passivity of surface functional groups, thus enhancing the ability of biochar to react with chemicals present in soil and water. As a result, biochar shows potential suitability as an adsorbent for cations and especially heavy metals. These differences in zeta levels based on feedstocks and biochar preparation conditions confirm the findings of previous studies [47,48].

Table 2. Chemical properties of biochars palm fronds (PFB) and sheep manure (SMB).

Chemical property	PFB		SMB	
	300°C	700°C	300°C	700°C
pH	6.44	9.72	7.82	10.7
EC ds m ⁻¹	6.41	16.3	7.6	8.2
Zeta Potential (mV)	-2.96	-8.39	-6.12	-8.01

3.9. Elemental Composition

The results of elemental analysis of PF and SM raw biomass are shown in Table 4. Elemental analyzes of PF and SM biochar. As the pyrolysis temperature increases (from 300°C to 700°C), the contents of hydrogen (H), nitrogen (N), sulfur (S), and oxygen (O) decrease, causing the loss in the above-mentioned elements. It is due to the decomposition and degradation of cellulose and the rest of the organic contents in the raw materials, including volatile substances [49]. Conversely, the carbon

content of biochar feedstock production gradually increased at the highest pyrolysis temperature, while zero percentage of sulfur (S) was found in PFB-700.

Although it is involved in pyrolysis, in addition, high-temperature treatment has shown a significant effect in increasing the carbon (C) content of biochar. Which may be a result of the decomposition of organic matter and the volatilization of many other elements, including H and O [10]. In short, C was diagnosed as an important component in all biochars, followed by O and some minor elements (N, H), Especially those that are produced at high temperatures. As well as with an increase in pyrolysis temperature, a decrease was observed in H/C, and O/C ratios among all biochars, which describe more carbon stability, hydrophobicity, and more aromaticity of the high temperatures that produce biochar, this was consistent with what was found [17].

The decrease in H/C molar ratios observed in both PFB and SMB chars with increasing pyrolysis temperature at 700 °C reflects the extent of biomass carbonization. A high H/C ratio indicates that biomass can be degraded or burned, making it an effective option for clean energy generation [50]. Moreover, the O/C ratio in biochar, which serves as an indicator of water density, indicates the presence of oxygen-containing functional groups, such as a carboxyl group [12].

Table 3. Element analysis of biochars palm fronds (PFB) and sheep manure (SMB).

W(%)	PFB		SMB	
	300 °C	700 °C	300 °C	700 °C
C (%)	58.34	62.4	52.47	59.18
H (%)	12.6	10.2	13.5	10.79
N(%)	14.6	10.57	8.76	7.95
S(%)	2.02	3.58	3.25	0
O(%)	12.46	13.25	22.02	22.08
H/C molar ratio	0.215	0.163	0.257	0.182
O/C molar ratio	0.213	0.212	0.419	0.373

3.10. The EDX Analysis

The (calcium, potassium, and phosphorus) elements in both biochar samples, PFB-300 and PFB-700, as shown in Table 5 revealed low levels. In contrast, the biochar derived from sheep manure (SMB-300 and SMB-700) showed acceptable levels of elements, allowing it to be used as a sustainable soil fertilizer. Significantly, a decrease in phosphorus levels from 3.24 to 1.24 was observed when the pyrolysis temperature increased from 300 to 700 degrees. The element content of biochar depends on the nature and quality of the raw materials, as well as the appropriate pyrolysis conditions (see Table 4). High temperatures during pyrolysis led to the volatilization of some elements, which is consistent with previous studies [51,52].

Table 4. EDX Shows the content of elements found in biochar.

Element(Wt)%	PFB		SMB	
	300°C	700°C	300°C	700°C
C	75.51	91.63	57.24	69.52
O	21.85	4.99	22.47	16.05
Si	0.06	0.0	6.81	1.38
P	0.00	0.00	3.42	1.24
Cl	0.19	1.07	0.44	1.69
K	0.84	1.23	3.02	3.13
Ca	0.89	0.71	6.41	6.12
Cd	0.12	0.07	0.00	0.00
Pb	0.54	0.24	0.17	0.83
Total,	100.00	100.00	100.00	100.00

Conclusion

This study concluded that the pyrolysis temperature affects both surface chemistry and physical properties. Pyrolysis of sheep manure produced biochar rich in stable aromatic carbon structures and essential inorganic minerals. Raising the pyrolysis temperature to 700°C enhanced the development of

pores, surface area and negative charge, making biochar adept at purifying water and soil by adsorbing cationic chemicals and organic pollutants. The surface of palm fronds biochar produced at 700°C pyrolysis (PFB-700) exhibits an exceptionally large surface area, surpassing other surfaces, and is distinguished by numerous cavities. With its highly negatively charged surface and rich abundance of functional groups, it emerges as a prime candidate for water and soil purification endeavors. Particularly noteworthy is its efficacy in removing heavy metals and facilitating water retention in soil. Biochar derived from plant fronds at 300°C exhibits acidic properties, which are advantageous for improving alkaline soils. Sheep manure biochar, subjected to pyrolysis at both 300°C and 700°C, may prove effective as a fertilizer for nutrient-deficient soils. However, it's worth noting that high pyrolysis temperatures may result in phosphorus volatilization and low total yield, underscoring the importance of opting for low-temperature biochar in such cases.

Conflict of Interest

The authors declared no conflict of interest in conducting this research.

Acknowledgement

The authors would like to thank University of Diyala – College of Agriculture for providing a research equipment's to conduct this research.

References

- [1] Zhang, W., Chen, R., Li, J., Huang, T., Wu, B., Ma, J., Wen, Q., Tan, J., & Huang, W. (2023). Synthesis optimization and adsorption modeling of biochar for pollutant removal via machine learning. *Biochar*, 5(1), 25.
- [2] Fahmi, A. H., Samsuri, A. W., & Singh, D. (2022). Magnetization improved fine particle biochar adsorption of Lead. *Soil and Sediment Contamination, An International Journal*, 31(5), 633-654.
- [3] Tan, X., Liu, Y., Zeng, G., Wang, X., Hu, X., Gu, Y., & Yang, Z. (2015). Application of biochar for the removal of pollutants from aqueous solutions. *Chemosphere*, 125, 70-85.
- [4] Yang, X., Zhang, S., Ju, M., & Liu, L. (2019). Preparation and modification of biochar materials and their application in soil remediation. *Applied Sciences*, 9(7), 1365.
- [5] Cayuela, M., Jeffery, S., & van Zwieten, L. (2015). The molar H, Corg ratio of biochar is a key factor in mitigating N₂O emissions from soil. *Agriculture, Ecosystems & Environment*, 202, 135-138.
- [6] Ahmad, M., Ishaq, M., Shah, W. A., Adnan, M., Fahad, S., Saleem, M. H., Khan, F. U., Mussarat, M., Khan, S., & Ali, B. (2022). Managing phosphorus availability from organic and inorganic sources for optimum wheat production in calcareous soils. *Sustainability*, 14(13), 7669.
- [7] Nartey, O. D., & Zhao, B. (2014). Biochar preparation, characterization, and adsorptive capacity and its effect on bioavailability of contaminants, an overview. *Advances in Materials Science and Engineering*, 2014.
- [8] Gonzaga, M. I. S., Matias, M. I. d. A. S., Andrade, K. R., de Jesus, A. N., da Costa Cunha, G., de Andrade, R. S., & de Jesus Santos, J. C. (2020). Aged biochar changed copper availability and distribution among soil fractions and influenced corn seed germination in a copper-contaminated soil. *Chemosphere*, 240, 124828.
- [9] Elkhilifi, Z., Iftikhar, J., Sarraf, M., Ali, B., Saleem, M. H., Ibranshabib, I., Bispo, M. D., Meili, L., Ercisli, S., & Torun Kayabasi, E. (2023). Potential role of biochar on capturing soil nutrients, carbon sequestration and managing environmental challenges, a review. *Sustainability*, 15(3), 2527.
- [10] Ippolito, J. A., Cui, L., Kammann, C., Wrage-Mönnig, N., Estavillo, J. M., Fuentetaja, T., Cayuela, M. L., Sigua, G., Novak, J., & Spokas, K. (2020). Feedstock choice, pyrolysis temperature and type influence biochar characteristics, a comprehensive meta-data analysis review. *Biochar*, 2, 421-438.
- [11] Baghdad, Iraq. (2022, 6 24). Retrieved from Iraqi Ministry of Agriculture, <https://www.zeraa.gov.iq>
- [12] Fahmi, A. H., Jol, H., & Singh, D. (2018). Physical modification of biochar to expose the inner pores and their functional groups to enhance lead adsorption. *RSC advances*, 8(67), 38270-38280.
- [13] Savova, D., Apak, E., Ekin, E., Yardim, F., Petrov, N., Budinova, T., Razvigorova, M., & Minkova, V. (2001). Biomass conversion to carbon adsorbents and gas. *Biomass and Bioenergy*, 21(2), 133-142.
- [14] Chen, B., Zhou, D., & Zhu, L. (2008). Transitional adsorption and partition of nonpolar and polar aromatic contaminants by biochars of pine needles with different pyrolytic temperatures. *Environmental science & technology*, 42(14), 5137-5143.

- [15] Song, W., & Guo, M. (2012). Quality variations of poultry litter biochar generated at different pyrolysis temperatures. *Journal of Analytical and Applied Pyrolysis*, *94*, 138-145.
- [16] Sun, H., Zhang, Y., & Zhang, W. (2013). Biochar and environment. In, Chemical Industry Press Beijing [in Chinese].
- [17] Almutairi, A. A., Ahmad, M., Rafique, M. I., & Al-Wabel, M. I. (2023). Variations in composition and stability of biochars derived from different feedstock types at varying pyrolysis temperature. *Journal of the Saudi Society of Agricultural Sciences*, *22*(1), 25-34.
- [18] Yuan, H., Lu, T., Huang, H., Zhao, D., Kobayashi, N., & Chen, Y. (2015). Influence of pyrolysis temperature on physical and chemical properties of biochar made from sewage sludge. *Journal of Analytical and Applied Pyrolysis*, *112*, 284-289.
- [19] Tsai, W.-T., Liu, S.-C., Chen, H.-R., Chang, Y.-M., & Tsai, Y.-L. (2012). Textural and chemical properties of swine-manure-derived biochar pertinent to its potential use as a soil amendment. *Chemosphere*, *89*(2), 198-203.
- [20] B, F. N., Zhang, X., Silva, L. C., Six, J., & Parikh, S. J. (2013). Use of chemical and physical characteristics to investigate trends in biochar feedstocks. *Journal of agricultural and food chemistry*, *61*(9), 2196-2204.
- [21] Tsai, W.-T., Jiang, T.-J., Lin, Y.-Q., Chang, H.-L., & Tsai, C.-H. (2021). Preparation of porous biochar from soapberry pericarp at severe carbonization conditions. *Fermentation*, *7*(4), 228.
- [22] Kavitha, B., Reddy, P. V. L., Kim, B., Lee, S. S., Pandey, S. K., & Kim, K.-H. (2018). Benefits and limitations of biochar amendment in agricultural soils, A review. *Journal of environmental management*, *227*, 146-154.
- [23] Zaini, M. A. A., Zhi, L. L., Hui, T. S., Amano, Y., & Machida, M. (2021). Effects of physical activation on pore textures and heavy metals removal of fiber-based activated carbons. *Materials Today, Proceedings*, *39*, 917-921.
- [24] Salem, I. B., El Gamal, M., Sharma, M., Hameedi, S., & Howari, F. M. (2021). Utilization of the UAE date palm leaf biochar in carbon dioxide capture and sequestration processes. *Journal of environmental management*, *299*, 113644.
- [25] Khadem, M., Husni Ibrahim, A., Mokashi, I., Hasan Fahmi, A., Noeman Taqui, S., Mohanavel, V., Hossain, N., Baba Koki, I., Elfasakhany, A., & Dhaif-Allah, M. A. (2023). Removal of heavy metals from wastewater using low-cost biochar prepared from jackfruit seed waste. *Biomass Conversion and Biorefinery*, *13*(16), 14447-14456.
- [26] Hu, X., Ding, Z., Zimmerman, A. R., Wang, S., & Gao, B. (2015). Batch and column sorption of arsenic onto iron-impregnated biochar synthesized through hydrolysis. *Water research*, *68*, 206-216.
- [27] Dilekoğlu, M. F. (2022). Malachite green adsorption from aqueous solutions onto biochar derived from sheep manure, adsorption kinetics, isotherm, thermodynamic, and mechanism. *International Journal of Phytoremediation*, *24*(4), 436-446.
- [28] Chen, J., Li, S., Huang, Q., Liu, H., Sun, J., Zhang, Y., & Lu, Y. (2022). Preparation of sheep manure biochar and its enhancement effect on wastewater treatment performance of CRI systems. MATEC Web of Conferences,
- [29] Boostani, H. R., Najafi-Ghiri, M., Hardie, A. G., & Khalili, D. (2019). Comparison of Pb stabilization in a contaminated calcareous soil by application of vermicompost and sheep manure and their biochars produced at two temperatures. *Applied Geochemistry*, *102*, 121-128.
- [30] Azeez, L., Oyefunke, O., Oyedeji, A. O., Agbaogun, B. K., Busari, H. K., Adejumo, A. L., Agbaje, W. B., Adeleke, A. E., & Samuel, A. O. (2024). Facile removal of rhodamine B and metronidazole with mesoporous biochar prepared from palm tree biomass, adsorption studies, reusability, and mechanisms. *Water Practice & Technology*, wpt2024049.
- [31] Alwan, Q. H., Rahman, A. M., Salman, M. H., & Ali, Z. H. (2015). Characterization of Biochar Produced from IRAQI Palm Fronds by Thermal Pyrolysis. *Al-Khwarizmi Engineering Journal*, *11*(2), 92-102.
- [32] Feng, Y., Zhao, D., Qiu, S., He, Q., Luo, Y., Zhang, K., Shen, S., & Wang, F. (2021). Adsorption of phosphate in aqueous phase by biochar prepared from sheep manure and modified by oyster shells. *ACS omega*, *6*(48), 33046-33056
- [33] Janu, R., Mrlik, V., Ribitsch, D., Hofman, J., Sedláček, P., Bielská, L., & Soja, G. (2021). Biochar surface functional groups as affected by biomass feedstock, biochar composition and pyrolysis temperature. *Carbon Resources Conversion*, *4*, 36-46..
- [34] Sizirici, B., Fseha, Y. H., Yildiz, I., Delclos, T., & Khaleel, A. (2021). The effect of pyrolysis temperature and feedstock on date palm waste derived biochar to remove single and multi-metals in aqueous solutions. *Sustainable Environment Research*, *31*, 1-16

- [35] Salem, I. B., Saleh, M. B., Iqbal, J., El Gamal, M., & Hameed, S. (2021). Date palm waste pyrolysis into biochar for carbon dioxide adsorption. *Energy Reports*, *7*, 152-159.
- [36] Brewer, C. E., Schmidt-Rohr, K., Satrio, J. A., & Brown, R. C. (2009). Characterization of biochar from fast pyrolysis and gasification systems. *Environmental progress & sustainable energy, an Official Publication of the American Institute of Chemical Engineers*, *28*(3), 386-396.
- [37] Ahmad, M., Lee, S. S., Dou, X., Mohan, D., Sung, J.-K., Yang, J. E., & Ok, Y. S. (2012). Effects of pyrolysis temperature on soybean stover-and peanut shell-derived biochar properties and TCE adsorption in water. *Bioresource technology*, *118*, 536-544.
- [38] Al-Wabel, M. I., Al-Omran, A., El-Naggar, A. H., Nadeem, M., & Usman, A. R. (2013). Pyrolysis temperature induced changes in characteristics and chemical composition of biochar produced from conocarpus wastes. *Bioresource technology*, *131*, 374-379.
- [39] Tomczyk, A., Sokołowska, Z., & Boguta, P. (2020). Biochar physicochemical properties, pyrolysis temperature and feedstock kind effects. *Reviews in Environmental Science and Bio/Technology*, *19*(1), 191-215.
- [40] Mukome, F. N., Zhang, X., Silva, L. C., Six, J., & Parikh, S. J. (2013). Use of chemical and physical characteristics to investigate trends in biochar feedstocks. *Journal of agricultural and food chemistry*, *61*(9), 2196-2204.
- [41] Tag, A. T., Duman, G., Ucar, S., & Yanik, J. (2016). Effects of feedstock type and pyrolysis temperature on potential applications of biochar. *Journal of Analytical and Applied Pyrolysis*, *120*, 200-206.
- [42] Hassan, M., Liu, Y., Naidu, R., Parikh, S. J., Du, J., Qi, F., & Willett, I. R. (2020). Influences of feedstock sources and pyrolysis temperature on the properties of biochar and functionality as adsorbents, A meta-analysis. *Science of The Total Environment*, *744*, 140714.
- [43] Cantrell, K. B., Hunt, P. G., Uchimiya, M., Novak, J. M., & Ro, K. S. (2012). Impact of pyrolysis temperature and manure source on physicochemical characteristics of biochar. *Bioresource technology*, *107*, 419-428.
- [44] Quilliam, R. S., Marsden, K. A., Gertler, C., Rousk, J., DeLuca, T. H., & Jones, D. L. (2012). Nutrient dynamics, microbial growth and weed emergence in biochar amended soil are influenced by time since application and reapplication rate. *Agriculture, Ecosystems & Environment*, *158*, 192-199.
- [45] Singh, B., Singh, B. P., & Cowie, A. L. (2010). Characterisation and evaluation of biochars for their application as a soil amendment. *Soil Research*, *48*(7), 516-525.
- [46] Gabhi, R. S., Kirk, D. W., & Jia, C. Q. (2017). Preliminary investigation of electrical conductivity of monolithic biochar. *Carbon*, *116*, 435-442..
- [47] Song, B., Chen, M., Zhao, L., Qiu, H., & Cao, X. (2019). Physicochemical property and colloidal stability of micron-and nano-particle biochar derived from a variety of feedstock sources. *Science of The Total Environment*, *661*, 685-695.
- [48] Hong, M., Zhang, L., Tan, Z., & Huang, Q. (2019). Effect mechanism of biochar's zeta potential on farmland soil's cadmium immobilization. *Environmental Science and Pollution Research*, *26*, 19738-19748
- [49] Usman, A. R., Abduljabbar, A., Vithanage, M., Ok, Y. S., Ahmad, M., Ahmad, M., Elfaki, J., Abdulazeem, S. S., & Al-Wabel, M. I. (2015). Biochar production from date palm waste, Charring temperature induced changes in composition and surface chemistry. *Journal of Analytical and Applied Pyrolysis*, *115*, 392-400.
- [50] Tripathi, M., Sahu, J. N., & Ganesan, P. (2016). Effect of process parameters on production of biochar from biomass waste through pyrolysis, A review. *Renewable and sustainable energy reviews*, *55*, 467-481.
- [51] Mohan, D., Sarswat, A., Ok, Y. S., & Pittman Jr, C. U. (2014). Organic and inorganic contaminants removal from water with biochar, a renewable, low cost and sustainable adsorbent—a critical review. *Bioresource technology*, *160*, 191-202.
- [52] Sakhiya, A. K., Anand, A., & Kaushal, P. (2020). Production, activation, and applications of biochar in recent times. *Biochar*, *2*, 253-285.